From Short Sample to Coil DC Superconductor Performance: ITER Central Solenoid Model Coil (CSMC) vs. Good Joint (GJ) Sample

L. Savoldi Richard, N. Mitchell, and R. Zanino

***Abstract*—The problem of how representative a short Nb_3Sn conductor sample is for simulating conductor-in-coil conditions in the ITER magnets is addressed here by considering the particular case of the Central Solenoid Model Coil (CSMC), tested in 2001–2003 at JAERI Naka, Japan, and its associated Good Joint (GJ) sample (tested in 1999 in the SULTAN facility). While the basic thermal-hydraulic conditions are interpreted from experimental data by the M&M code, the sensitivity of the voltage-temperature characteristics to mechanical effects (due to the strain sensitivity of the Nb_3Sn) is investigated by analysis. The results are used to assess the errors to be expected in predicting coil performance from measurements made on conductor samples.**

***Index Terms*—Fusion reactors, ITER, modeling, superconducting coils.**

TABLE I
MAIN CONDUCTOR PARAMETERS (FROM [9])

	CS1.4 (GJ)	CS1.1 (CSMC)
Strand diameter (mm)	0.81	
Number of strands	1152	
Cu : non Cu ratio	1.495	1.490
Cabling pattern	3×4×4×4×6	
Nominal pitches (mm)	50/105/152/ 260/393	25/53.5/95.3/ 147/397
Nominal void fraction	36.3%	
Jacket material	Incoloy	
Jacket outer size (mm)	51×51	
Average J_C @ 4.2 K, 12 T (A/mm^2)	637	593

I. INTRODUCTION

ONE OF THE crucial problems for the design of the large high field superconducting magnets of the International Thermonuclear Experimental Reactor (ITER), using Nb_3Sn superconductors, is how to extrapolate from the performance of an isolated strand to the performance of the superconducting coil. The strand performances are typically measured on isolated strands in controlled field and temperature conditions. On the contrary, the performance of a coil, which is made by more than a thousand strands twisted with a complex multi-stage pattern, is measured in tests where the magnetic field has always a significant gradient (order 0.1–1 T) on the conductor cross section, and the temperature cannot be measured exactly at the location where the superconductor critical condition appears first [1], [2]. There is also usually a significant tensile strain due to magnetic forces that is not present in a strand test.

The uncertainty in the extrapolation from strand to coil performance can be covered by generous margins, but of course this implies a cost penalty. Within the frame of the ITER activities, it is proposed to bridge this extrapolation gap through the test of short (few meter long) but full-size well-instrumented conductor samples in dedicated facilities, e.g., SULTAN at Villigen PSI, Switzerland. However, the issue of how representative the short conductor sample is of the conditions of a (long) conductor in an ITER coil is still under discussion. A possible answer to this problem comes from the comparison of the performances of the ITER Model Coils, namely the Toroidal Field Model Coil (TFMC) [3] and the Central Solenoid Model Coil (CSMC) [2], with those of the respective short samples (the TFMC Full Size Joint Sample (FSJS) [4] and the Good Joint (GJ) [5]) and strands—Europa Metalli (EM) LMI for the TFMC and VacuumSchmelze (VAC) for the CSMC.

Here we concentrate on the comparison VAC vs. GJ vs. CSMC. The strand performances are described by the interpolative scaling law from [6]. The analysis of the conductor sample performance will be based on the experimental data, while for the coil the analysis will be performed with the M&M code [7], using in input the results of a new mechanical model of the cable.

The comparison LMI vs. TFMC FSJS vs. TFMC has been already presented in a companion paper [8].

II. ANALYSIS OF THE GOOD JOINT PERFORMANCE

The GJ sample [5] was made with two straight sections (leg A and B) of the CSMC high field conductor, leftover after the winding of the fourth layer of the CSMC (CS1.4). The two identical conductor legs, jointed at their bottom with a hairpin joint, were heat treated before joining. After the heat treatment, which was comparable to that of the CSMC, leg B was bent and re-straightened. The sample, cooled with supercritical helium (SHe) at ~1 GPa and 4.5 K, was tested in the SULTAN facility in 1999 during three different test campaigns (length of the joint reduced from the original 400 mm down to 320 mm and to 280 mm). The main conductor data are reported in Table I.

We use the critical current (I_C) tests at a background field of 9 T and 11 T, performed during the first test campaign on leg A, for the GJ performance assessment (the somewhat worse

Manuscript received September 20, 2005. This work was supported in part by EFDA and MIUR.

L. S. Richard and R. Zanino are with Dipartimento di Energetica, Politecnico, Torino, Italy (e-mail: laura.savoldi@polito.it).

N. Mitchell is with ITER IT, Naka, Japan.

Digital Object Identifier 10.1109/TASC.2006.873259

1051-8223/$20.00 © 2006 IEEE

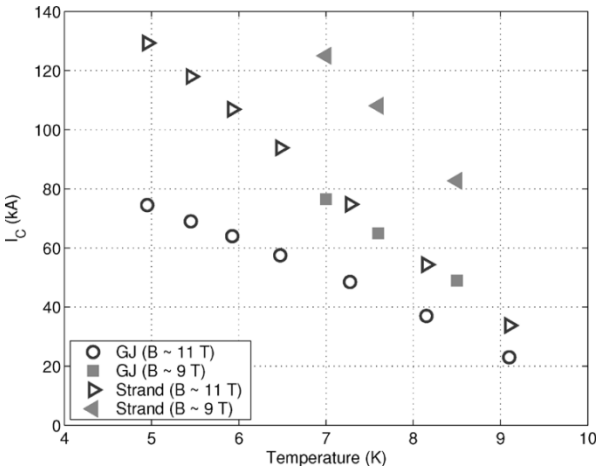

Fig. 1. GJ critical current as a function of the temperature at a background field ∼11 T (open symbols) and ∼9 T. The average self-field ($3.85 \times 10^{-6} \times \mathrm{I_C}$) has been accounted for in the evaluation of the strand performance.

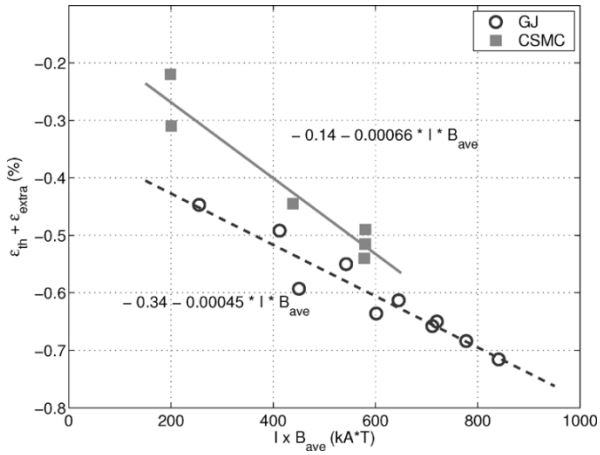

Fig. 2. Thermal plus extra strain as a function of the magnetic load, computed at the average field, for the GJ (open circles) and for the CSMC (squares).

performance of leg B [5] will not be analyzed here). The signal from the voltage taps across the high field region, symmetrically located with respect to the SULTAN field axis and ∼0.5 m apart, is smoothed with a 10 pts moving average and base-lined to zero. The electric field-transport current (E–I) characteristic is then used to deduce $\mathrm{I_C}$, corresponding to an average electric field $\mathrm{E(voltage/length)} = \mathrm{E_C} = 10\ \mu\mathrm{V/m}$.

The sample $\mathrm{I_C}$, measured at different temperatures, is reported in Fig. 1, together with the strand $\mathrm{I_C}$, evaluated at the average magnetic field $\mathrm{B_{ave}}$ (on the cable axis), and at a strain of -0.32% [2]. Note that the Durham interpolative scaling for the VAC strand performance foresees an average $\mathrm{J_C}$ of 631 $\mathrm{A/mm^2}$ at 4.2 K and 12 T fully consistent with the average $\mathrm{J_C}$ of the sample conductor, see Table I.

A clear degradation, with respect to the strand performance, is present at all temperature levels, but it gets lower at higher temperature (lower current). This degradation can be presented in terms of the fitting parameter $\varepsilon_{\mathrm{extra}}$ [2], [3], to be added to the thermal and operational longitudinal strain on the superconducting filaments.

$$\varepsilon_{\mathrm{tot}} = \varepsilon_{\mathrm{th}} + \varepsilon_{\mathrm{op}} + \varepsilon_{\mathrm{extra}} \tag{1}$$

where $\varepsilon_{\mathrm{tot}}$ is used in the evaluation of the critical current $\mathrm{I_C} = \mathrm{I_C(T, B, \varepsilon_{tot})}$. For the present it will be assumed that loads applied to the cable from the jacket (whether operational or thermal) appear 100% on the strands. This means that the cable shows no flexibility due to bending [10], an approximation that is discussed later.

Fig. 2 presents the correlation between $\varepsilon_{\mathrm{th}} + \varepsilon_{\mathrm{extra}}$ and the magnetic load. $\varepsilon_{\mathrm{extra}}$ (considered uniform across and along the conductor) is computed to best-fit the reduction of performance in Fig. 1 at $\mathrm{B_{ave}}$. As the load increases, the degradation becomes higher. This confirms the behavior observed first on the later Model Coil tests [2], [3], which went unnoticed at the time of the GJ test.

The linear extrapolation to conditions with zero load would allow in principle the estimation of the thermal strain $\varepsilon_{\mathrm{th}}$, which seems to roughly confirm the value assumed for the analysis (-0.34% vs. -0.32%).

III. Improved Mechanical Model of the CSMC Conductor

Cables in curved jackets have an enhanced operating strain once the circular geometry is taken into account, compared to expectations based on the analysis only of the jacket behavior. This is due to the outward movement of the cable within the jacket combined with the relatively low longitudinal stiffness of the cable compared to the supporting structures (mostly the jacket). In a previous assessment, an analytical approach was used to derive approximate values for this strain, which were then used to reassess the coil superconducting performance [8].

As already discussed in [8] the nonlinearity of the displacement-force dependence in these cables makes an analytical or numerical approach difficult. Therefore the corrections to the longitudinal strain arising from the transverse compression of the cable to one side of the jacket [8] have been computed here using an approach based on mechanical measurements of the transverse modulus of the cable [11].

The overall transverse modulus $\mathrm{E_x}$ (i.e., the slope of a line joining the origin to the point on the curve) is shown in Figs. 3 and 4 as a function of displacement and transverse force, respectively. To be consistent with the typical number of cycles experienced by the CSMC, the data after 100 load cycles has been used here. Besides the CS1 conductor, two samples of the TFMC conductor (A and B) were also tested and the corresponding data, see also [8], are shown in the plots (samples TFMC-A and B are from the same cable to check variability). Fig. 4 shows that the log-log plot for forces F∼10 kN/m is linear (i.e., there is a power law relationship between $\mathrm{E_x}$ and F). Also quite striking, the power law exponent is very similar for all 3 samples and is quite close to 1. It is not clear if there is any significance to this, but it allows a convenient assessment of the cable performance under transverse loads.

The model presented here is based on the simplified scaling developed from the finite element calculation [8] (with $\varepsilon_{\mathrm{extra}}$ inversely proportional to $\mathrm{E_x}$ and the local radius of curvature).

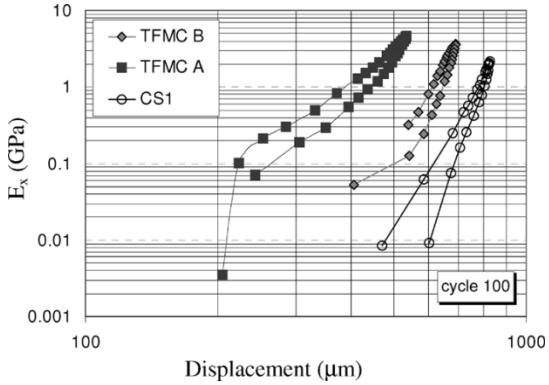

Fig. 3. Transverse modulus of cables as function of displacement (with blocked maximum cable relaxation) (data provided by University of Twente [11], [12]). Modulus is overall value, stress/strain, not local $\mathrm{d}\sigma/\mathrm{d}\varepsilon$.

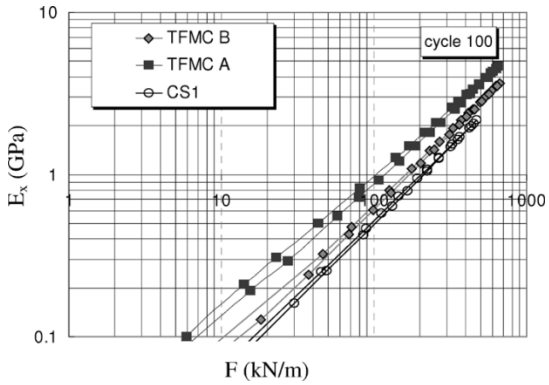

Fig. 4. Transverse modulus of cables as function of load (with blocked maximum cable relaxation). Data provided by University of Twente [11], [12].

From Fig. 4 (and using the transverse stress$\sigma = \mathrm{F}/\mathrm{c}$ instead of F, with $\mathrm{c} =$ effective cable width)

$$\mathrm{E_x} = \mathrm{A}\ \sigma^{\mathrm{p}} \tag{2}$$

where A and p are fitting parameters.

An essential assumption in what follows is that the local behavior inside a cable at a given local stress is the same as the overall measured behavior, as this allows the mechanical test (external force) to be related to the magnetic loading case (distributed forces).

The transverse stress is given by

$$\sigma = \mathrm{Bjx} \tag{3}$$

where $\mathrm{j} = \mathrm{I}/\mathrm{c}^2$ is the current density (c is the equivalent cable width, assuming a square cable with the same cross section), and x is the transverse (radial) coordinate in the cable, measured from the inboard surface.

$\varepsilon_{\mathrm{local}}$ is the local strain

$$\varepsilon_{\mathrm{local}} = \frac{\mathrm{d}\delta}{\mathrm{dx}} = \frac{(\mathrm{Bjx})}{\mathrm{A}\sigma^{\mathrm{p}}} \tag{4}$$

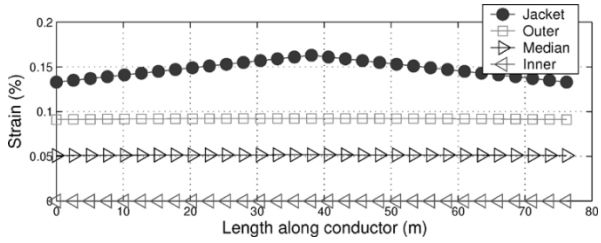

Fig. 5. Extra strain contribution in CSMC conductor 1 A @ 46 kA.

where δ is the transverse displacement

$$\delta = \left(\frac{\mathrm{F_o^p}}{\mathrm{cE_{xo}}}\right)(\mathrm{BI})^{(1-\mathrm{p})}(2\mathrm{r})\left(\frac{1}{(2-\mathrm{p})}\right)\left(1-\left(\frac{\mathrm{x}}{2\mathrm{r}}\right)^{(2-\mathrm{p})}\right) \tag{5}$$

$\mathrm{F_o}$ is the force (N/m) at which the transverse overall modulus is $\mathrm{E_{xo}}$ in the Twente data, and r is the cable radius (i.e., the total distance from inboard to outboard surface is 2r). From Fig. 4, $\mathrm{p} = 0.818$. Thus, the dependence of δ on the local value of BI is rather weak, being to the power 0.182. However the variation of δ from inner surface to outer (where $\delta = 0$) is almost linear (power 1.182). This reflects the very low modulus as low loads are applied to the cable.

There is also a permanent settlement δ_{p} in the cable over the first few load cycles that can be seen in Fig. 3. This is presumably due to plastic deformation of the strands. However, there is no data available on how this permanent settlement varies across the cable section. A variation that is proportional to the elastic part of the displacement δ has been assumed, on the basis that local plasticity occurs immediately with any mechanical or magnetic loading, due to the initial thermal stresses [10].

Using these expressions it is possible to find the resulting longitudinal strain anywhere in the cable.

$$\varepsilon_{\mathrm{tot}} = \varepsilon_{\mathrm{th}} + \varepsilon_{\mathrm{op}} + \frac{(\delta + \delta_{\mathrm{p}})}{\mathrm{R}} \tag{6}$$

where R is the local radius of curvature and δ is the local transverse displacement. The longitudinal modulus should be included for a complete analysis. However, the cable is so flexible compared to the jacket that its longitudinal stiffness makes only a small contribution to supporting the transverse magnetic load (i.e., if only the cable supported the magnetic loads without the jacket the radial displacement would be much larger than δ).

Equation (6) can be used to calculate the extra strain in the CSMC cable section, as shown in Fig. 5, compared to the jacket operating strain.

IV. Analysis of the CSMC Performance

The re-assessment of the CSMC performance using the new mechanical model and local $\varepsilon_{\mathrm{extra}}$ has been performed with the M&M code under the assumption of uniform current distribution [8], using the same setup as in [2] for the three current levels of 46 kA, 40 kA and 30 kA. Since the Durham scaling [6] overestimates the average $\mathrm{J_C}$ on the CS1.1 conductor, see Table I,

TABLE II
SUMMARY OF THE RESULTS OF THE CSMC PERFORMANCE ANALYSIS

I (kA)	Run #	n	ε_{extra} (%)	T_{st} at 10 μV/m (K)	y at 10 μV/m (m)	B_{ave} at T_{CS} (T)
46	038-002	**6**	**–0.16%**	7.27	46.7	12.6
		8	**–0.18%**	7.16	45.2	12.6
	020-002	**5**	**–0.18%**	7.19	45.1	12.6
		8	**–0.21%**	7.02	45.2	12.6
	090-002	**6**	**–0.22%**	7.00	42.4	12.6
		7	**–0.22%**	6.99	42.4	12.6
40	041-002	**5**	**–0.11%**	8.76	42.4	11.0
		5	**–0.14%**	8.67	37.5	11.0
30	051-002	**4**	**0.02%**	12.01	6.6	6.8
		5	**0.00%**	12.17	5.0	6.6
	092-002	**4**	**0.12%**	12.48	4.0	6.5
		6	**0.08%**	12.28	5.5	6.7

the critical current density fit has been rescaled by a factor of 0.94 in order to account for this effect.

The results, in terms of $\varepsilon_{\mathrm{extra}}$ and n-value (exponent in the conductor E-j power-law characteristic [2]) are reported in Table II as a function of the average magnetic load $(\mathrm{I_{TFMC}} \times \mathrm{B_{ave}})$ at the location y along the conductor where the current sharing temperature $\mathrm{T_{CS}}$ is reached for the first time, together with the value of $\mathrm{T_{CS}} (= \mathrm{T_{st}}$ at 10 $\mu \mathrm{V/m})$, for the different runs. In Fig. 2 the total strain is reported as a function of the magnetic load (computed as current × average field at the location were $\mathrm{T_{CS}}$ is reached first). If compared to the previous analysis performed with the Summers critical scaling law and reported in [2], the slope of the linear best-fit of the computed points is ∼40% lower. Including the strain profile (5), (6) on the conductor cross section results in slightly more negative $\varepsilon_{\mathrm{extra}}$ than if a uniform value of the strain is assumed.

From any monotonic extrapolation of the best-fit curve in Fig. 2 back to zero load, it is clear that the thermal strain, appears here to be lower than the quoted value of -0.32% (in the case of linear extrapolation, $\sim -0.14\%$).

This is obviously physically unlikely, so we need to look for an explanation in our original assumptions. The most obvious of these is that the strain (both from differential contraction and operation loads) is not transmitted 100% to the cable. Recent work [13] suggests that a cable 'equivalent flexibility factor' of 80% would be appropriate. This would affect the curves in Fig. 2: the CSMC line would become less steep and the expected thermal strain would be $0.8 \times (-0.32\%) \sim -0.25\%$.

V. SAMPLE VS. COIL COMPARISON

Coming to the comparison between the sample and the coil in terms of total strain, form Fig. 2 one can see that the sample appears to be conservative, with respect to the coil, at least in the range of magnetic load of the CSMC tests. The loss of performance of the CSMC shows, however, a somewhat (∼50%) higher slope than for the sample.

The difference in the slopes would be reduced with a reduced jacket—cable strain bonding [13]. However the overall high level of the CSMC performance is not explainable unless, e.g., differences in the nominally similar heat treatment were assumed. The possible role of current nonuniformity in the seemingly different performance of coil vs. sample (Fig. 2) will be addressed elsewhere.

ACKNOWLEDGMENT

The authors would like to thank M. Bagnasco for running the M&M simulations.

REFERENCES

[1] R. Zanino *et al.*, "Performance evaluation of the ITER toroidal field model coil phase I. Part 1: current sharing temperature measurement," *Cryogenics*, vol. 43, pp. 79–90, 2003.
[2] ——, "Analysis and interpretation of the full set (2000–2002) of Tcs tests in conductor 1 A of the ITER central solenoid model coil," *Cryogenics*, vol. 43, pp. 179–197, 2003.
[3] R. Zanino and L. Savoldi Richard, "Performance evaluation of the ITER toroidal field model coil phase I. Part 2: M&M analysis and interpretation," *Cryogenics*, vol. 43, pp. 91–100, 2003.
[4] D. Ciazynski *et al.*, "Test results and analysis of two European full-size conductor samples for ITER," *IEEE Trans. Appl. Supercond.*, vol. 10, pp. 1058–1061, 2000.
[5] P. Bruzzone, "Manufacture and performance results of an improved joint for the ITER conductor," *Adv. Cryo. Eng.*, vol. 45, pp. 737–744, 2000.
[6] S. A. Keys and D. Hampshire, "A scaling law for the critical current density of weakly and strongly-coupled superconductors, used to parametrise data from a technological $\mathrm{Nb_3Sn}$ strand," *Supercond. Sci. Technol.*, vol. 16, pp. 1097–1108, 2003.
[7] L. Savoldi and R. Zanino, "M&M: multi-conductor Mithrandir code for the simulation of thermal-hydraulic transients in super-conducting magnets," *Cryogenics*, vol. 40, pp. 179–189, 2000.
[8] R. Zanino *et al.*, "Coupled mechanical-electromagnetic-thermal-hydraulic effects in $\mathrm{Nb_3Sn}$ cable-in-conduit conductors for ITER," *Supercond. Sci. Technol.*, vol. 18, pp. S376–S382, 2005.
[9] "Database of CSMC and CS Insert," JAERI memo 12-046, Mar. 2000.
[10] N. Mitchell, "Mechanical and magnetic load effects in $\mathrm{Nb_3Sn}$ cable-in-conduit conductors," *Cryogenics*, vol. 43, no. 3–5, pp. 255–270, 2003.
[11] A. Nijhuis *et al.*, "Performance of an ITER CS1 model coil conductor under transverse cyclic loading up to 40 000 cycles," *IEEE Trans. Appl. Supercond.*, vol. 14, pp. 1489–1494, 2005.
[12] A. Nijhuis, *Data from limited void fraction measurements in the Twente Press.* July 2005, private communication.
[13] N. Mitchell, "Assessment of conductor degradation in the ITER CSI coil and implications for the ITER conductors," ITER Internal Report, Sep. 2005.